Effect of the gap width in AZ31 magnesium alloy joints obtained by friction stir welding

Chiuzuli, Fernanda Rocha; Batistão, Bruna Fernanda; Bergmann, Luciano Andrei; Alcântara, Nelson Guedes de; dos Santos, Jorge Fernandez; Klusemann, Benjamin; Gargarella, Piter

Published in:
Journal of Materials Research and Technology

DOI:
10.1016/j.jmrt.2021.10.115

Publication date:
2021

Document Version
Publisher's PDF, also known as Version of record

Available online at www.sciencedirect.com

jmr&t Journal of Materials Research and Technology

journal homepage: www.elsevier.com/locate/jmrt

Original Article

Effect of the gap width in AZ31 magnesium alloy joints obtained by friction stir welding

Fernanda Rocha Chiuzuli [a], *Bruna Fernanda Batistão* [a,*], *Luciano Andrei Bergmann* [b], *Nelson Guedes de Alcântara* [a,c], *Jorge Fernandez dos Santos* [b], *Benjamin Klusemann* [b,d], *Piter Gargarella* [a,c,e]

[a] *Federal University of Sao Carlos, Graduate Program in Materials Science and Engineering (PPGCEM/UFSCar), Rodovia Washington Luiz, Km 235 SP-310, 13565-905, São Carlos, São Paulo, Brazil*

[b] *Helmholtz-Zentrum Hereon, Institute of Materials Mechanics, Solid State Materials Processing, Max-Planck-Str. 1, 21502, Geesthacht, Germany*

[c] *Federal University of Sao Carlos, Department of Materials Engineering (DEMa/UFSCar), Rodovia Washington Luiz, Km 235 SP-310, 13565-905, São Carlos, São Paulo, Brazil*

[d] *Leuphana University of Lüneburg, Institute of Product and Process Innovation, Universitätsallee 1, 21335, Lüneburg, Germany*

[e] *Center of Characterization and Development of Materials (CCDM), Federal University of Sao Carlos, Rodovia Washington Luiz, Km 235 SP-310, 13565-905, São Carlos, São Paulo, Brazil*

ARTICLE INFO

Article history:
Received 24 August 2021
Accepted 26 October 2021
Available online 5 November 2021

Keywords:
AZ31
Mg alloy
Lightweight material
Friction stir welding
Butt joint configuration
Gap width

ABSTRACT

Thin AZ31 magnesium alloy sheets, i.e., 2 mm thick, are welded by Friction Stir Welding (FSW) in butt joint configuration using gap width up to 1.15 mm. All welds present good surface finishing and no internal defects, except for the weld produced using the maximum gap width. A reduction of the weld thickness within the Stir Zone is seen with the increase in gap width, leading to a maximum thickness reduction of 8.5%. Microstructure and Vickers hardness investigations reveal no influence of the gap width on these properties. Up to a gap width of 0.51 mm, a slight decrease in the Ultimate Tensile Strength (UTS) is observed with increasing gap width. For larger gap widths, the UTS, as well as the fracture strain, are constant. To keep the metallurgical integrity, a maximum gap width of 1 mm seems acceptable for joints of thin AZ31 magnesium alloy sheets produced by FSW.

1. Introduction

The high strength-to-weight ratio of magnesium alloys has made them promising candidates for structural applications in the automotive and aerospace industries [1,2]. The most commonly used magnesium alloy AZ31 contains aluminum and zinc as alloying elements [3]. The presence of aluminum enhances the hardness, corrosion resistance, and tensile strength through the formation of the intermetallic $Mg_{17}Al_{12}$

* Corresponding author.
E-mail address: brunafbatistao@gmail.com (B.F. Batistão).
https://doi.org/10.1016/j.jmrt.2021.10.115

phase. The zinc favors the formation of fine grains during solidification and increases tensile strength, which has led to high interest in AZ31 as structural alloys, especially for automotive applications [4].

For the application of AZ31, different welding processes have been investigated, such as Tungsten Inert Gas [5], Resistance Spot Welding [6–8], and Laser Beam Welding [9–11]. However, joining magnesium alloys via fusion welding techniques is a difficult task due to the poor weldability of the alloy, caused by porosity formation and hot cracking in the weld zones [12,13]. To avoid such defects, the application of these processes requires the complete elimination of the workpieces' surface oxide layer and high purity shielding gases because of the high reactivity of magnesium at high temperatures [12]. As a consequence, solid-state welding processes, such as Friction Stir Welding (FSW) [1,12,14–18] and refill Friction Stir Spot Welding (refill FSSW) [19–21], are a very suitable alternative to join AZ31 or to process lightweight alloys, such as the titanium-based alloys processed by Friction Stir Processing (FSP) for implants [22,23], due to the lower process temperature, i.e., below the melting point of the materials, which avoids the previously mentioned problems related to solidification [24].

FSW was developed in 1991 at The Welding Institute (TWI) and consists of the insertion and traverse movement of a rotating non-consumable tool, composed of a pin and a shoulder, along with the contact interface of the workpieces. The main probe functions are to heat, plasticize and mix the material by friction, and the main shoulder functions are to generate additional heating by friction and to avoid the extrusion of the plasticized material out of the weld zone. Thus, the friction between the tool and the material to be welded generates the necessary heat to plasticize the materials, and the combination of tool traverse and rotating movement leads to the movement of materials, resulting in a joint produced in solid-state [25–27].

Considering the mechanical of this process, two different sides can be determined. The Advancing Side (AS) is the side where welding and rotational speed are in agreement, and the Retreating Side (RS) is the side where these two parameters are in opposite directions. The temperature distribution and material flow pattern during the welding affect the microstructural and mechanical properties of the joints produced by FSW, which are influenced by the tool geometry, joint design, and process parameters, such as probe insertion depth, tool rotational speed, welding speed, axial force, and tilt angle [25–27]. The thermal field and strain rate are also influenced by the material properties, such as thermal conductivity [27,28].

Gulati et al. [14] analyzed the influence of the probe geometry on the formation of defect-free welds in FSW of AZ31 and showed that voids and tunnel defects are reduced when decreasing the welding speed and using a truncated tool profile in comparison with a cylindrical tool profile. Various authors examined the influence of the welding and rotational speed on microstructure and texture distribution since a preferential crystallographic orientation can be generated in the Stir Zone (SZ) and Thermo-Mechanically Affected Zone (TMAZ), which strongly affect the mechanical properties of the welds [1,12,13,15–18]. The development of a very strong {0001} <*uvtw*> β-fiber basal texture in the SZ was observed by Mironov et al. [15] investigating the effect of welding temperature through the variation of the welding speed on the grain structure evolution during FSW of AZ31. As discussed by Suhuddin et al. [13], the basal planes of AZ31 tend to align parallel with the surface column of the probe in FSW due to the shear deformation induced by the rotating probe, which results in the (0002) plane perpendicular to the welding direction in the SZ center. Chowdhury et al. [1] investigated the orientation of the basal planes in the SZ. This orientation is significantly reduced at low welding speed and high rotational speed, which leads to a high temperature in the SZ, and consequently to complete dynamic recrystallization and no preferred grain orientations. Moreover, Xin et al. [16] showed that differences in the texture between SZ and TMAZ may result in fracture at the interface SZ/TMAZ during tensile tests of AZ31 FSW welds, which confirmed results of earlier studies by Commin et al. [17] and Pareek et al. [12]. Commin et al. [17] and Xuhong et al. [18] also demonstrated an increase in the microhardness in the SZ due to grain refinement as a result of low SZ temperature with the rotational speed decrease and welding speed increase.

However, none of these studies addresses the possible effects of disturbances, such as gaps between the abutting edges of the workpieces, which may occur by improper manufacturing or clamping of the material to be welded. To avoid rejection and rework of the workpieces, which would consume time and generate additional costs, it is important to gain knowledge of the gap tolerance to produce welds without joint strength degradation [29–31]. In this regard, Ma et al. [29] showed that the heat generation and material flow in FSW of 6.2 mm thick 2A14-T6 aluminum alloy joints are affected by the gap width. A significant decrease in joint efficiency appears when the gap exceeds 1.6 mm, so roughly 25% of the plate thickness. Similarly, the influence of the gap width on macrostructure and mechanical properties of AA5083 welds produced by FSW was analyzed by Tsarkov et al. [30] and Cole et al. [31], which obtained a maximum gap of 20% of sheets thickness as the threshold before a significant decrease in tensile strength was present. Nevertheless, the effect of the gap width on AZ31 welds has not been reported so far.

In this regard, the main objective of the present study is the analysis of the effect of the gap width on the microstructural and mechanical properties of AZ31 magnesium alloy joints produced by FSW and the evaluation of possible gap tolerances to produce welds without joint strength degradation. The microstructural characteristics were evaluated to verify the presence of defects and identify the weld zones. The Vickers hardness and tensile tests were done in order to evaluate the global mechanical performance of the joint and correlate them with the different offsets.

2. Materials and methods

2.1. *Friction Stir Welding procedure*

Rolled AZ31 magnesium alloy sheets (140 mm wide, 475 mm long, and 2 mm thick), with a nominal chemical composition (wt.%) of 2.5–3.5% Al, 0.20–1.0% Mn, 0.6–1.4% Zn and the

balance Mg (ASTM B90/B90M–15), represent the base material used in this study. The workpieces were brushed and cleaned with acetone before welding to remove oxides and grease. The tool is composed of a triflate and threaded conical probe with a diameter of 5 mm and a length of 1.8 mm, and a flat scrolled shoulder with a diameter of 13 mm.

The welding procedure was carried out perpendicular to the rolling direction using a high stiffness FSW Gantry System machine. The samples were welded in butt joint configuration with different gap widths between the sheets, as shown in Fig. 1. The welding process was performed position controlled, where the tool rotational speed of 2000 rpm, welding speed of 2 m/min, and tilt angle of 0.5° were kept constant. The targeted gap width was varied from 0.00 mm up to 0.90 mm, as summarized in Table 1. The gap width was set up using rigid spacers with specific thickness positioned between the abutting edges of the workpieces along the entire sheets length. After fixture of the sheets, the spacers were removed before welding, where only spacers were kept near the in- and outlet zones. The real gap width during the welding process was measured by the Micro-Epsilon scanCONTROL® 2960-10 laser, located in front of the probe, see Fig. 1(c). In general, the measured gap width was almost constant along the welding direction. The welds with set gaps of 0.1, 0.3, and 0.5 mm presented a slight increase in the measured gap width near the end of the weld. The average measured real gap width, summarized in Table 1, was always higher than the initially set gap width. The reason is associated with the process forces that act on the workpieces pushing them apart and resulting in an almost constant real gap width during the welding process.

2.2. *Joint characterization*

The welds were sectioned perpendicularly to the welding direction for the microstructural and mechanical characterization. For the microstructural analyses, the welded samples were mechanical grounded, polished, and chemical etched using a solution of 2–3 g of picric acid, 6.5–7.0 mL of acetic acid, 30–40 mL of distilled water, and 140 mL ethanol, with 4 s of immersion. The micrographs were examined via a Leica SM

Table 1 – Initially set (via spacers) and measured (via laser) gap width for each welding trial. The weld name indicates the measured gap width.

Weld	Set Gap (Spacers) (mm)	*Real Gap* (mm)
GC00	0.00	0.00
GC21	0.05	0.21 ± 0.09
GC30	0.10	0.30 ± 0.05
GC51	0.30	0.51 ± 0.08
GC83	0.50	0.83 ± 0.03
GC98	0.70	0.98 ± 0.06
GC115	0.90	1.15 ± 0.05

IRM® optical microscope equipped with polarized light, and the grain sizes were determined using the ASTM E112-13 standard throughout the intercept method.

Vickers hardness measurements were conducted horizontally along the cross-section of the welds in the thickness centerline using a Struers DuraScan® hardness machine. A load of 100 g for 10 s was used with 0.25 mm distance between each measurement position.

Tensile tests in a screw-driven Zwick/Roell® testing machine with a load capacity of 100 kN were performed at room temperature and at a crosshead speed of 1 mm/min to evaluate the static mechanical properties. Three tensile specimens were prepared and tested according to DIN 50125 with a gauge length of 50 mm for the base material and each welding condition.

3. Results

Photographs and optical macrographs of welds obtained with different gap widths are shown in Figs. 2 and 3, respectively. In Fig. 2 weld surfaces of GC21 and GC115 can be seen, and in Fig. 3 the macrostructure of some welds cross-sections is shown. Except for the weld with a gap width of 1.15 mm, all further welds present good surface finishing, as exemplarily shown in Fig. 2(a) for a gap width of 0.21 mm. For a gap width of 1.15 mm, lack-of-fill defect on the weld surface is identified, Fig. 2(b). Besides that, no defects such as voids and cracks are

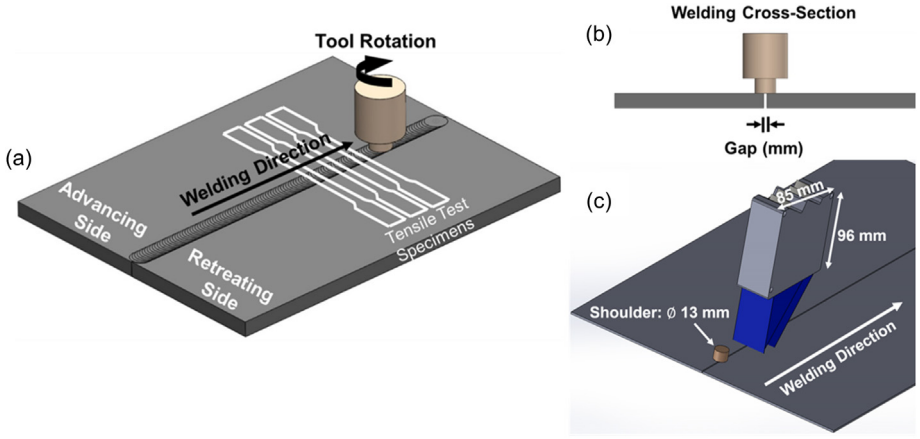

Fig. 1 – Schematic illustration of the (a) welding configuration, (b) welding cross-section, and (c) laser positioning, with the blue surface indicating the laser.

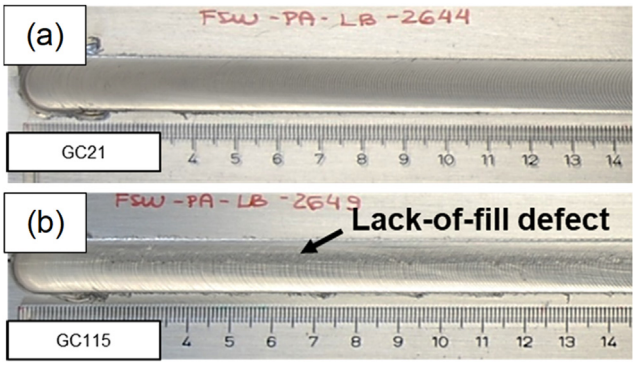

Fig. 2 – Photographs of the welds produced with a real gap width of (a) 0.21 mm and (b) 1.15 mm.

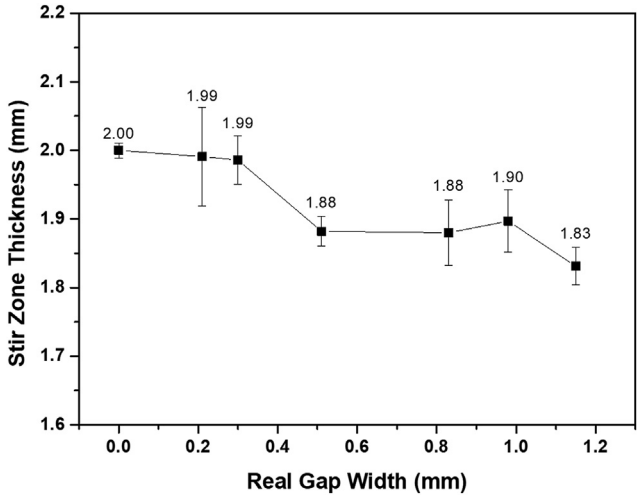

Fig. 4 – Measured thickness in the Stir Zone (SZ) after welding in relation to the measured (real) gap width.

observed in all macrostructures of the weld cross-sections, see four examples in Fig. 3.

Considering the possibility of thickness decreasing within the SZ due to the welding process, the weld thickness of all samples was obtained, and these thickness variations are shown in Fig. 4. An increase in the gap width results in a decrease in the thickness of the weld within the SZ. As it should be, FSW with 0.0 mm gap width leads to a joint thickness of 2 mm, representing the material thickness of the sheet material, where the thickness decreases by 8.5% to 1.83 mm for a 1.15 mm gap, see Fig. 4.

In terms of microstructure, the different regions of the FSW can be divided as usual into SZ, TMAZ, Heat Affected Zone (HAZ), and Base Material (BM), see Fig. 5(a). The AZ31 BM, Fig. 5(b), is characterized by equiaxed grains of different sizes, containing lenticular-shaped twins, resulting from the deformation imposed by the rolling process. A similar grain structure is observed in the HAZ, Fig. 5(c), but with an increased number of annealing twins. In the TMAZ, dynamic recrystallization occurred, i.e. finer and equiaxed grains are observed, Fig. 5(d). The SZ, Fig. 5(e), presents mainly equiaxed and recrystallized grains, which are homogeneously distributed.

Independently of the gap width variation, the microstructure of the SZ exhibited approximately the same grain size in the welds, between 9.1 μm and 10.5 μm, as can be observed in Fig. 6 and Table 2. Compared to the BM grain size of 20 ± 3 μm, the SZ presented a finer microstructure due to the dynamic recrystallization induced by the FSW process.

The dissymmetrical material flow in FSW results in two different transition regions from HAZ to SZ. Figure 7 shows the differences between the AS and RS. The transition from HAZ to SZ on the RS, Fig. 7(a), is wider and less sharp than on the AS, and the microstructure presents fewer lenticular-shaped twins in the HAZ and a higher concentration of dynamically recrystallized grains in the TMAZ.

The influence of the microstructure of the different regions of the welds in the hardness profile is shown in Fig. 8. Similar hardness profiles and average SZ hardness (Table 2) were observed for the welds, which is a result of the similar microstructures in the welds produced with different real gap

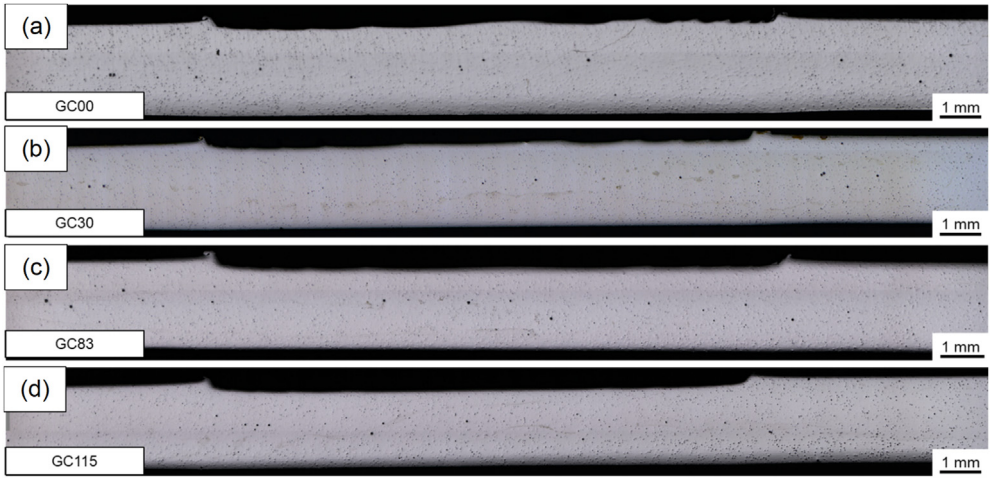

Fig. 3 – Macrostructure of the welds produced with a real gap width of (a) 0.00 mm, (b) 0.30 mm, (c) 0.83 mm, and (d) 1.15 mm.

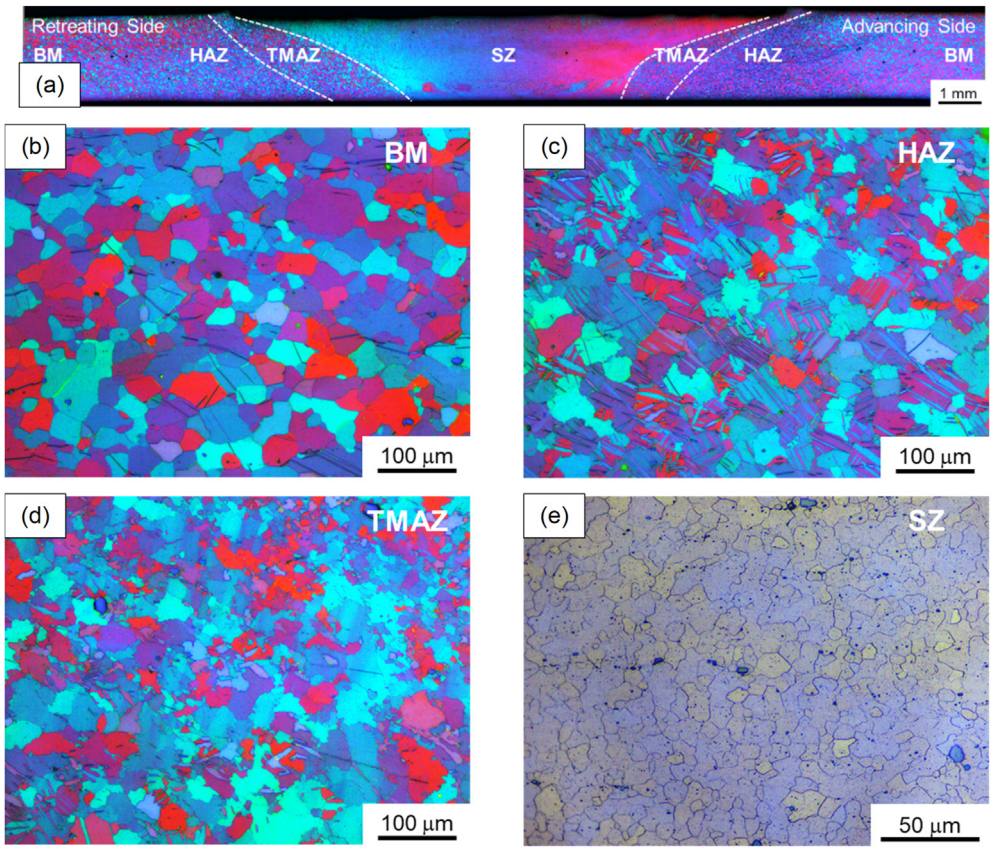

Fig. 5 – (a) Micrograph of a weld produced with a real gap width of 0.30 mm: (b) Base Material (BM), (c) Heat Affected Zone (HAZ), (d) Thermo-Mechanically Affected Zone (TMAZ), and (e) Stir Zone (SZ).

widths. The SZ presents similar values of hardness to the BM of around 57 HV_{01}, as well as the HAZ. The maximum hardness of approximately 70 HV_{01} is obtained in the TMAZ at the RS.

The influence of the gap width on the mechanical properties of the welds is summarized in Fig. 9(a). The Ultimate Tensile Strength (UTS) of the welds is calculated using the individual SZ thickness for each sample, see Fig. 4. A slight decrease in the UTS is observed with the increase of the gap width up to 0.51 mm. For larger gap width, the UTS, as well as the fracture strain, are almost constant. Moreover, the tensile test resulted in similar fracture for all welds, which occurred in the weld region as shown in Fig. 9(b).

4. Discussion

During the FSW with a gap, the plasticized material flows to the space created by the gap, which reduces the volume of material being deformed by the probe. Consequently, this leads to a lack of material to fill the top of the weld surface, resulting in a lack-of-fill defect when a high gap width is used, as in the case of the weld produced with a gap width of 1.15 mm, Fig. 2(b). Besides that, a decrease in thickness of the weld within the SZ is observed with the increase of the gap width, see Fig. 4. This occurred because the volume of material being deformed and transported by the tool decreases with increasing gap width. Since plasticized material fills the cavity left by the probe from the bottom to the top of the weld, the lack of material occurs only at the top of the weld, resulting in the thickness reduction in the SZ. Despite the reduction of material being transported by the tool, the plasticized material was enough to fill the cavity left by the probe without the formation of internal defects, as shown in Fig. 3. No lack-of-fill defect is observed for gap widths below 1.15 mm, although these gap widths led even to the thickness reduction of up to 6%, see Fig. 4. Overall, the metallographic analyses indicate that a gap size of up to 1 mm, representing 50% of the sheet thickness, still leads to a stable process without surface defects in the current study.

In terms of microstructure, in AZ31 the twinning modes are also important for the plastic deformation of magnesium alloys, being most common the observation of $\{10\bar{1}2\}$ twins, normally nucleated at grain boundaries and preexisting twin boundaries, and propagated to the other side of the grain [32]. As a result, equiaxed grains of different sizes containing lenticular-shaped twins are observed in the BM and HAZ, Fig. 5(b) and Fig. 5(c), due to the deformation imposed by the previous rolling process.

The twins present in the BM and HAZ disappear in the TMAZ due to the transformation of the low angle twin boundaries into high angle boundaries during dynamic

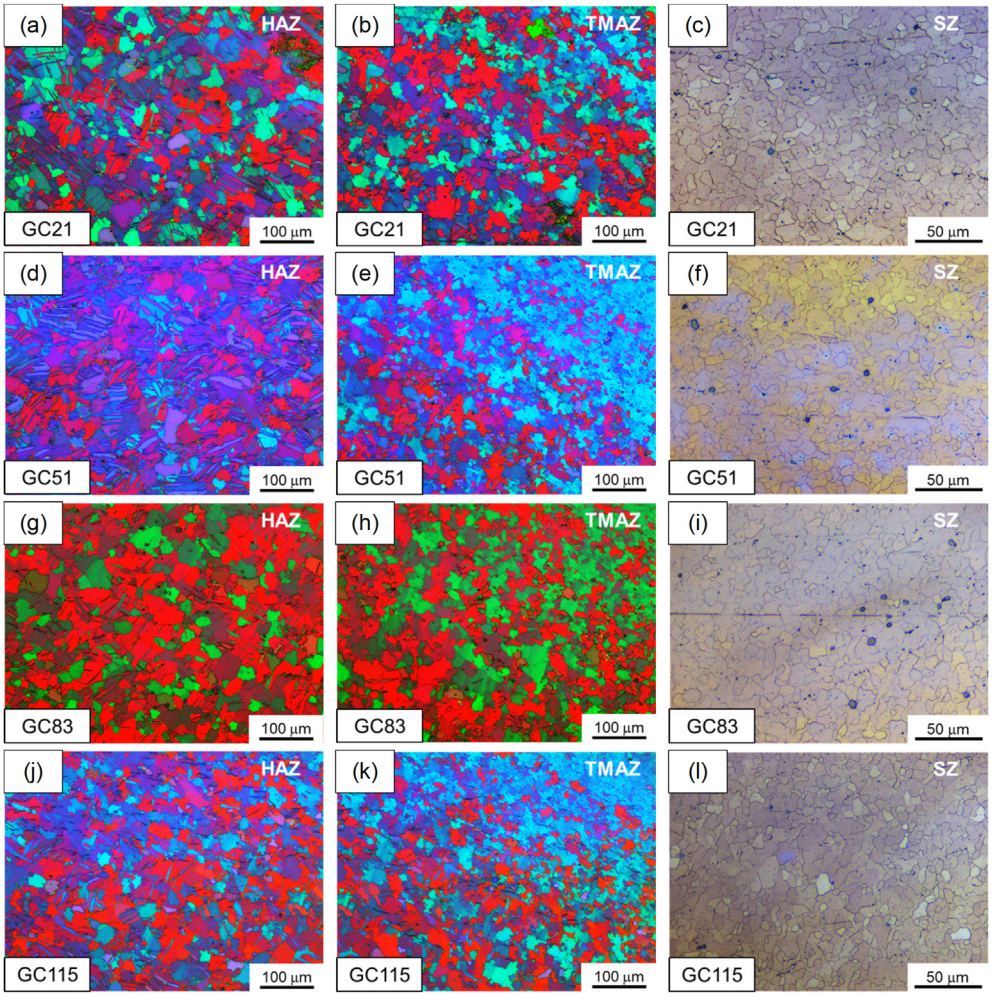

Fig. 6 – Heat Affected Zone (HAZ), Thermo-Mechanically Affected Zone (TMAZ) and Stir Zone (SZ) of weld produced with a real gap width of (a–c) 0.21 mm (d–f) 0.51 mm (g–i) 0.83 mm, and (j–l) 1.15 mm. The same welding speed and rotational speed were used for these samples.

recrystallization, as reported by Polmear et al. [32], resulting in finer and equiaxed grains in the TMAZ, Fig. 5(d). The SZ, Fig. 5(e) and Fig. 6, presents a fine microstructure with equiaxed and recrystallized grains resultant from the plastic deformation and frictional heating during FSW, as discussed by Singh et al. [27]. Similar grain sizes in the SZ between 9.1 μm and 10.5 μm were obtained for AZ31 processed by FSW reported in the literature [33].

The mentioned microstructural differences result from the different levels of severe plastic deformation and frictional heat introduced by the rotating probe and shoulder in each weld zone. The deformation mechanisms and microstructure evolution are typically affected by the temperature (initial) grain orientation (texture) and size, solute atoms, and second-phase particles [32], which in turn determine the mechanical properties of the joints. For example, the SZ temperature can be estimated by Equation (1), where T_m is the alloy melting point, α and K are constants, ω is the rotational speed and υ is the welding speed [17]. Therefore, since the welding parameters (ω and υ), tool size, and geometry are the same for all joints, the gap width did not significantly affect the plastic deformation and frictional heating during the FSW process, and for all welding samples similar microstructures are present, as shown in Fig. 6. At this way, in terms of gap width, no reportable effect on the different microstructural zones, as well as in SZ grain size, Table 2, can be determined.

Table 2 – SZ grain size and average hardness of the welded samples.

Weld	SZ grain size (μm)	SZ Vickers Hardness (HV)
GC00	10.1 ± 0.3	58.3 ± 1.3
GC21	9.1 ± 0.8	57.2 ± 1.8
GC30	10.3 ± 1.2	56.3 ± 1.4
GC51	9.7 ± 1.5	56.9 ± 2.1
GC83	10.5 ± 1.3	58 ± 2
GC98	9.1 ± 1.2	58.1 ± 1.8
GC115	9.8 ± 1.3	58.0 ± 1.6

$$\frac{T}{T_m} = K\left(\frac{\omega^2}{\upsilon \times 10^4}\right)^{\alpha} \quad (1)$$

In Fig. 7, the transition region from HAZ to SZ presents characteristic differences between the AS and RS caused by

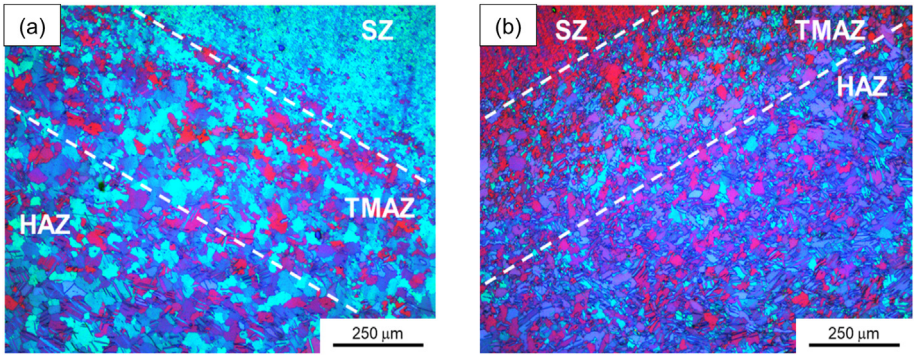

Fig. 7 – Transition from Stir Zone (SZ) to Heat Affected Zone (HAZ) on the (a) Retreating (RS) and (b) Advancing Side (AS) of the weld for a sample with a real gap width of 0.30 mm.

the dissymmetrical material flow. At the RS, the welding direction is opposite to the tangent tool rotation, which results in two opposing forces acting on the plasticized material, that is the forward force produced by the traverse tool movement and the backward force produced by the rotational tool that transfers the material to the back of the tool on the RS [12]. These opposite forces result in higher straining and temperature at the RS, which contribute to dynamic recrystallization.

Despite the gap width variation, all joints show similar hardness profiles, see Fig. 8, confirming that the gap width has no effect on the heat input and plastic deformation of the material, and that the microstructure kept similar for all welds independent of gap width. As discussed by Heidarzadeh et al. [28], in magnesium alloys the grain refinement has a stronger effect on the overall hardness than precipitation strengthening. Thus, since a finer microstructure is observed in the SZ, and smaller grains result in more grain boundaries and obstacles to the slip of dislocations, the hardness in the SZ should be higher than of the BM, nevertheless, the typical magnesium alloys {0001} <*uwtv*> β-fiber texture produces a soft region in the SZ, reducing its hardness values, as reported by Chowdhury et al. [1], resulting in similar values of hardness

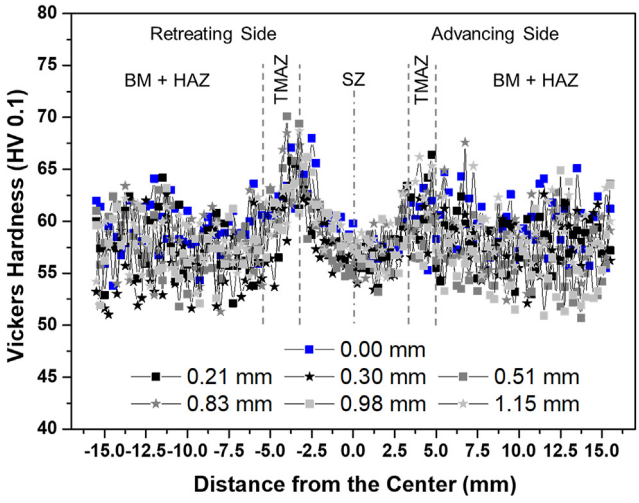

Fig. 8 – Vickers hardness profile of the welds produced with different real gap widths.

in the SZ and BM. The dominant mechanism of deformation of the magnesium and its alloys, which have a hexagonal closed packed crystal structure, is the {0001} basal slip. However, due to the limited number of basal slip systems, non-basal slip may occur at room temperature, that is the {112} <11$\bar{2}$3> pyramidal slip and {10$\bar{1}$0} <1$\bar{2}$10> prismatic slip, but in favorable orientations or higher stresses [32]. The hardness in the HAZ is similar to the BM, indicating no relevant influence of the increased number of annealing twins. The maximum hardness is obtained in the TMAZ due to the presence of finer recrystallized grains compared to the BM, and weaker preferential crystallographic orientation than in the SZ, as reported by Liu et al. [34]. The maximum hardness occurred in the TMAZ at the RS, where the straining and temperature are higher than at the AS, which enhances the dynamic recrystallization process.

Regarding the mechanical properties of the welds, with increasing gap width, the UTS and the fracture strain slightly decreases, see Fig. 9(a), where a gap width of 1.15 mm leads to approximately 79% of the UTS of the BM, which is consistent with results reported in the literature on FSW of AZ31 [1,12,18]. Moreover, the tensile test resulted in the fracture of the welds in the weld zone, as also observed by Afrin et al. [35] for FSW of AZ31, where the samples presented a 45° shear fracture, similar to that in Fig. 9(b), between the SZ and the TMAZ. The fracture in the weld zone, between the SZ and the TMAZ, is reported by some authors [34–36] to be resultant of the maximum accumulation of the basal slip plane (0001) at the boundary between the SZ and the TMAZ leading to the minimum Schmid factor, with the normal direction of these planes parallel to the transverse direction, and that the incompatibility of plasticity of the SZ and the TMAZ may cause the fracture at the boundary between the zones.

Studies conducted by Ma et al. [29], Tsarkov et al. [30], and Schultz et al. [37] explored the mechanical performance of welds by FSW with gaps. The three studies analyzed the UTS for maximum gap values of 2 mm. Ma et al. [29] similarly found the constancy of UTS with gaps up to 1.15 mm, since their welds with gaps until 0.8 mm showed a slow decrease in UTS values and significant reductions for gaps from 1.6 to 2.0 mm. Similarly, Schutz et al. [37] also presented almost constant UTS values for gap values up to approximately 1 mm,

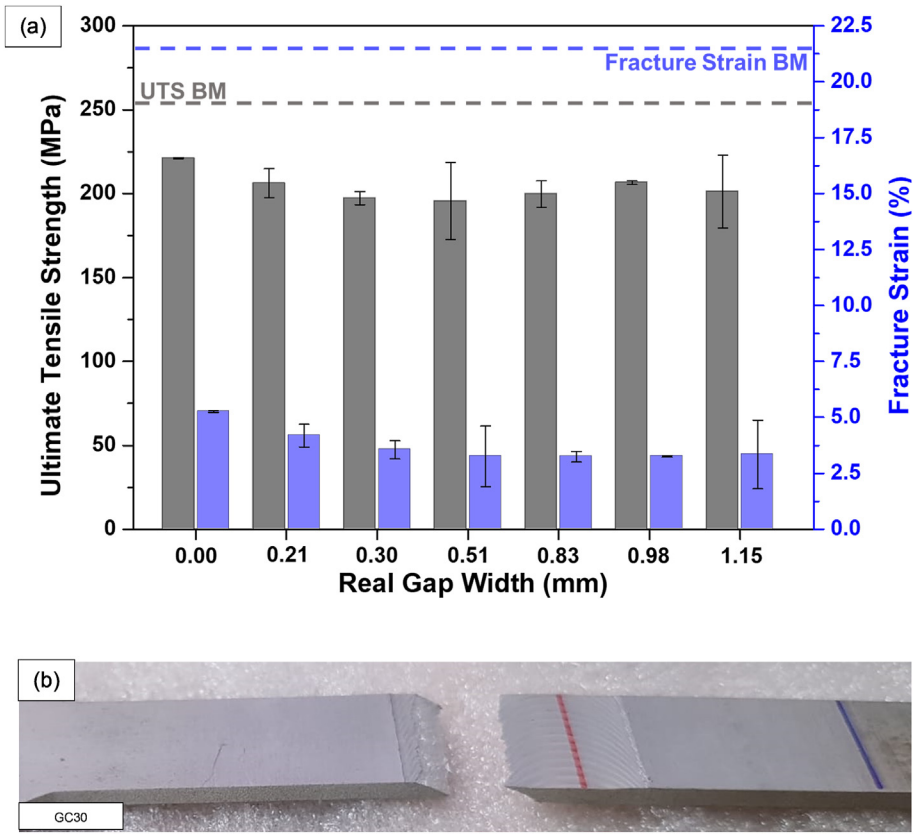

Fig. 9 – (a) Effect of the gap width between the sheets on Ultimate Tensile Strength and fracture strain of the welds, and (b) fracture region in sample GC30 after tensile test.

and considerable reduction for larger gaps. Tsarkov et al. [30] suggested the FSW tolerance for gaps of 20% of the plate thickness, being discrepant values when compared with the tolerance achieved in this study of approximately 50% of the thickness.

Based on these results, it is concluded that the mechanical properties of AZ31 magnesium alloy FSW welds are maintained with increasing gap width, only for a gap width of 1.15 mm a surface defect is observed. Therefore, it is concluded that metallurgical and mechanical integrity of the welds can only be ensured up to a maximum gap width of approximately 1 mm, representing 50% of the BM thickness. A larger gap width results in too significant SZ thickness reduction, i.e. higher than 6%, which causes the formation of surface defects, due to the lack of material to fill the cavity left by the probe in the weld zone.

5. Conclusions

AZ31 magnesium alloys joints produced by FSW with different gap widths up to 1.15 mm were investigated. The microstructural and mechanical analyses of the welds provided the following results and conclusion:

- The welds present good surface finishing and no internal defects, except for the weld produced with the maximum gap width of 1.15 mm, which exhibited a lack-of-fill defect on the top surface. The flow of plasticized material to the gap during the process resulted in a reduction of the weld thickness within the SZ, which increases with gap width. A maximum thickness reduction of 8.5% within the SZ is obtained for the maximum gap width, resulting in the lack-of-fill defect on the top surface.
- The rolled BM microstructure is characterized by equiaxed grains of different sizes, containing lenticular-shaped twins. A similar microstructure is observed in the HAZ, with an increasing number of annealing twins. These twins disappear in the TMAZ, and some finer grains were formed due to dynamic recrystallization. The dynamic recrystallization was enhanced in the SZ, resulting in even finer and equiaxed grains.
- The maximum hardness of around 70 HV_{01} is obtained in the TMAZ due to the presence of fine grains. Since the gap width did not significantly affect the plastic deformation and frictional heat during the FSW process, the microstructure of the weld zones and their hardness values are similar in all joints investigated. Only a slight decrease in the UTS and fracture strain is observed with increasing gap width.
- To keep the metallurgical integrity of the welds without the formation of the lack-of-fill defect, a maximum gap width of 50% of BM thickness is recommended for AZ31 magnesium alloy joints produced by FSW of 2 mm thick sheets, using the process parameters chosen in this study.

Declaration of Competing Interest

The authors declare that they have no known competing financial interests or personal relationships that could have appeared to influence the work reported in this paper.

Acknowledgements

This study was financed in part by the support of the Coordenação de Aperfeiçoamento de Pessoal de Nível Superior – Brasil (CAPES) – Finance Code 001. The authors also thank the grant #2019/04613–3, São Paulo Research Foundation (FAPESP).

REFERENCES

[1] Chowdhury SH, Chen DL, Bhole SD, Cao X, Wanjara P. Friction stir welded AZ31 magnesium alloy: microstructure, texture, and tensile properties. Metall Mater Trans 2013;44:323–36. https://doi.org/10.1007/s11661-012-1382-3.

[2] Yuan W, Mishra RS. Grain size and texture effects on deformation behavior of AZ31 magnesium alloy. Mater Sci Eng, A 2012;558:716–24. https://doi.org/10.1016/j.msea.2012.08.080.

[3] Powell BR, Krajewski PE, Luo AA. Magnesium alloys for lightweight powertrains and automotive structures. In: Mallick PK, editor. Materials, design and manufacturing for lightweight vehicles. Woodhead Publishing Ltd; 2010. p. 114–73. https://doi.org/10.1533/9781845697822.1.114.

[4] Acharya MG, Shetty AN. The corrosion behavior of AZ31 alloy in chloride and sulfate media – a comparative study through electrochemical investigations. J Magnes Alloy 2019;7:98–112. https://doi.org/10.1016/j.jma.2018.09.003.

[5] Wen T, Liu S, Chen S, Liu L, Yang C. Inlfuence of high frequency vibration on microstructure and mechanical properties of TIG welding joints of AZ31 magnesium alloy. Trans Nonferrous Met Soc China 2015;25:397–404. https://doi.org/10.1016/S1003-6326(15)63616-0.

[6] Kishore Babu N, Brauser S, Rethmeier M, Cross CE. Characterization of microstructure and deformation behaviour of resistance spot welded AZ31 magnesium alloy. Mater Sci Eng, A 2012;549:149–56. https://doi.org/10.1016/j.msea.2012.04.021.

[7] Wang YR, Mo ZH, Feng JC, Zhang ZD. Effect of welding time on microstructure and tensile shear load in resistance spot welded joints of AZ31 Mg alloy. Sci Technol Weld Join 2007;12:671–6. https://doi.org/10.1179/174329307X238380.

[8] Wang YR, Feng JC, Zhang ZD. Microstructure characteristics of resistance spot welds of AZ31 Mg alloy. Sci Technol Weld Join 2006;11:555–60. https://doi.org/10.1179/174329306X128446.

[9] Quan YJ, Chen ZH, Gong XS, Yu ZH. Effects of heat input on microstructure and tensile properties of laser welded magnesium alloy AZ31. Mater Char 2008;59:1491–7. https://doi.org/10.1016/j.matchar.2008.01.010.

[10] Gao M, Wang H, Hao K, Mu H, Zeng X. Evolutions in microstructure and mechanical properties of laser lap welded AZ31 magnesium alloy via beam oscillation. J Manuf Process 2019;45:92–9. https://doi.org/10.1016/j.jmapro.2019.07.001.

[11] Hao K, Wang H, Gao M, Wu R, Zeng X. Laser welding of AZ31B magnesium alloy with beam oscillation. J Mater Res Technol 2019;8:3044–53. https://doi.org/10.1016/j.jmrt.2019.04.024.

[12] Pareek M, Polar A, Rumiche F, Indacochea JE. Metallurgical evaluation of AZ31B-H24 magnesium alloy friction stir welds. J Mater Eng Perform 2007;16:655–62. https://doi.org/10.1007/s11665-007-9084-5.

[13] Suhuddin UFHR, Mironov S, Sato YS, Kokawa H, Lee CW. Grain structure evolution during friction-stir welding of AZ31 magnesium alloy. Acta Mater 2009;57:5406–18. https://doi.org/10.1016/j.actamat.2009.07.041.

[14] Gulati P, Shukla DK, Gupta A. Defect formation analysis of friction stir welded magnesium AZ31B alloy. Mater Today Proc 2017;4:1005–12. https://doi.org/10.1016/j.matpr.2017.01.113.

[15] Mironov S, Onuma T, Sato YS, Kokawa H. Microstructure Evolution during friction-stir welding of AZ31 magnesium alloy. Acta Mater 2015;100:301–12. https://doi.org/10.1016/j.actamat.2015.08.066.

[16] Xin R, Liu D, Shu X, Li B, Yang X, Liu Q. Influence of welding parameters on texture distribution and plastic deformation behavior of as-rolled AZ31 Mg alloys. J Alloys Compd 2016;670:64–71. https://doi.org/10.1016/j.jallcom.2016.02.023.

[17] Commin L, Dumont M, Masse JE, Barrallier L. Friction stir welding of AZ31 magnesium alloy rolled sheets: influence of processing parameters. Acta Mater 2009;57:326–34. https://doi.org/10.1016/j.actamat.2008.09.011.

[18] Xunhong W, Kuaishe W. Microstructure and properties of friction stir butt-welded AZ31 magnesium alloy. Mater Sci Eng, A 2006;431:114–7. https://doi.org/10.1016/j.msea.2006.05.128.

[19] Luo T, Shi B, Duan Q, Fu J, Yang Y. Fatigue behavior of friction stir spot welded AZ31 Mg alloy sheet joints. Trans Nonferrous Met Soc China 2013;23:1949–56. https://doi.org/10.1016/S1003-6326(13)62682-5.

[20] Yin YH, Sun N, North TH, Hu SS. Hook formation and mechanical properties in AZ31 friction stir spot welds. J Mater Process Technol 2010;210:2062–70. https://doi.org/10.1016/j.jmatprotec.2010.07.029.

[21] Yuan W, Mishra RS, Carlson B, Verma R, Mishra RK. Material flow and microstructural evolution during friction stir spot welding of AZ31 magnesium alloy. Mater Sci Eng, A 2012;543:200–9. https://doi.org/10.1016/j.msea.2012.02.075.

[22] Wang L, Xie L, Lv Y, Zhang LC, Chen L, Meng Q, et al. Microstructure evolution and superelastic behavior in Ti-35Nb-2Ta-3Zr alloy processed by friction stir processing. Acta Mater 2017;131:499–510. https://doi.org/10.1016/j.actamat.2017.03.079.

[23] Wang L, Qu J, Chen L, Meng Q, Zhang LC, Qin J, et al. Investigation of deformation mechanisms in β-type Ti-35Nb-2Ta-3Zr alloy via FSP leading to surface strengthening. Metall Mater Trans 2015;46:4813–8. https://doi.org/10.1007/s11661-015-3089-8.

[24] Moraes JFC, Rodriguez RI, Jordon JB, Su X. Effect of overlap orientation on fatigue behavior in friction stir linear welds of magnesium alloy sheets. Int J Fatig 2017;100:1–11. https://doi.org/10.1016/j.ijfatigue.2017.02.018.

[25] Mishra RS, Ma ZY. Friction stir welding and processing. Mater Sci Eng R 2005;50:1–78. https://doi.org/10.1016/j.mser.2005.07.001.

[26] Çam G, Mistikoglu S. Recent developments in friction stir welding of Al-alloys. J Mater Eng Perform 2014;23:1936–53. https://doi.org/10.1007/s11665-014-0968-x.

[27] Singh K, Singh G, Singh H. Review on friction stir welding of magnesium alloys. J Magnes Alloy 2018;6:399–416. https://doi.org/10.1016/j.jma.2018.06.001.

[28] Heidarzadeh A, Mironov S, Kaibyshev R, çam G, Simar A, Gerlich A, et al. Friction stir welding/processing of metals

and alloys: a comprehensive review on microstructural evolution. Prog Mater Sci 2021;117:100752. https://doi.org/10.1016/j.pmatsci.2020.100752.

[29] Ma H, Wang Y, Tian Z, Xiong L, Zhang Y. Gap-tolerance control for friction stir butt welding of 2A14 aluminum alloy. Measurement 2019;148:1–13. https://doi.org/10.1016/j.measurement.2019.106915.

[30] Tsarkov A, Trukhanov K, Zybin I. The influence of gaps on friction stir welded AA5083 plates. Mater Today Proc 2019;19:1869–74. https://doi.org/10.1016/j.matpr.2019.07.030.

[31] Cole EG, Fehrenbacher A, Shultz EF, Smith CB, Ferrier NJ, Zinn MR, et al. Stability of the friction stir welding process in presence of workpiece mating variations. Int J Adv Manuf Technol 2012;63:583–93. https://doi.org/10.1007/s00170-012-3946-1.

[32] Polmear I, StJohn D, Nie JF, Qian M. Light alloys. 5th ed. Elsevier; 2017.

[33] Padmanaban G, Balasubramanian V. Selection of FSW tool pin profile, shoulder diameter and material for joining AZ31B magnesium alloy – an experimental approach. Mater Des 2009;30:2647–56. https://doi.org/10.1016/j.matdes.2008.10.021.

[34] Liu D, Xin R, Zhao L, Hu Y. Effect of textural variation and twinning activity on fracture behavior of friction stir welded AZ31 Mg alloy in bending tests. J Alloys Compd 2017;693:808–15. https://doi.org/10.1016/j.jallcom.2016.09.187.

[35] Afrin N, Chen DL, Cao X, Jahazi M. Microstructure and tensile properties of friction stir welded AZ31B magnesium alloy. Mater Sci Eng 2008;472:179–86. https://doi.org/10.1016/j.msea.2007.03.018.

[36] Woo W, Choo H, Brown DW, Liaw PK, Feng Z. Texture variation and its influence on the tensile behavior of a friction-stir processed magnesium alloy. Scripta Mater 2006;54:1859–64. https://doi.org/10.1016/j.scriptamat.2006.02.019.

[37] Shultz EF, Cole EG, Smith CB, Zinn MR, Ferrier NJ, Pfefferkorn FE. Effect of compliance and travel angle on friction stir welding with gaps. J Manuf Sci Eng 2010;132:041010. https://doi.org/10.1115/1.4001581.